On the Turbulent Boundary Layer with Pressure Rise and Fall.

By Busuke Hudimoto.

This paper contains results from both experiments and computations.

The first part covers the experimental results of the velocity distributions of turbulent boundary layers in diverging and converging channels. To express the varying forms of these velocity distributions, the following empirical formula is proposed.

$$u=u_0 g\left(\frac{y}{\delta}\right)\left\{m+(1-m)\,h\left(\frac{y}{\delta}\right)\right\},$$

where u is the velocity at distance y from the surface of the wall, δ is the thickness of the boundary layer and u_0 is the velocity at $y=\delta$ or at the outer boundary of the layer.

As the function of $g\left(\frac{y}{\delta}\right)$, the form of velocity distribution in a parallel wall channel or along a flat plate placed edgewise to the stream is taken. Then $h\left(\frac{y}{\delta}\right)$ is a function of $\frac{y}{\delta}$, which is obtained from the experimental results and shown in Figs. 6 aud 10 in the original paper.

Some considerations on the back flow in a diverging channel are suggested. As the result it was found that the back flow may occur on one side of the wall at a smaller diverging angle than is the case of back flow on both sides, the ratio of these angles being about 0.5.

As applications of the above formula of the velocity distribution, problems of turbulent boundary layer of figure of revolution and approximate relations between the Reynolds' number and maximum lift coefficient of aerofoil section are treated, making use of Gruschwitz's empirical formula.

The theory of turbulent boundary layer was first investigated by Th. v. Kármán[1] and L. Prandtl[2], and many other theories and results of experiments have been published since then. They have treated mainly the flow along a flat plate placed edgewise to the stream, or in a straight pipe. In these cases the pressure gradient is equal to zero or a constant respectively. But generally the flow of fluid is accompanied with a pressure rise or fall or, more strictly speaking a change of velocity in the direction of flow. In such cases, if the flow in the boundary layer is laminar, calculation is theoretically possible. Several papers have been published discussing them. But owing to complications arising in the turbulent flow, there are few results obtained by experiments and no theory is plausible.

On the present phase of this subject there are available experimental results of E. Gruschwitz[3] and A. Buri[4] on the turbulent boundary layer, and those of Fr. Dönch[5], J. Nikuradse[6] and others on the turbulent flow in diverging and converging channels. In the following sections, results of experiments are presented; and making use of Gruschwitz's empirical formula, possibilities of solving some problems of turbulent boundary layers are mentioned.

1. Experiments on the Flow in Diverging and Converging Channels.

On the turbulent flow in diverging and converging channels, there are elaborate experimental results by Dönch and Nikuradse. The present experiments were carried out in the same way as those of these two authors, at the Tyûô-Zikkenzyo of the Kyôto Teikoku Daigaku during the summer of 1933 and supplimentary tests in 1934.[7]

The arrangements of the experiments are shown in Fig. 1. A small ventilator V delivers air into the channel A_1 and in passing through A_1 and A_2 turbulency of the stream is settled down by the honey comb H and screens of fine mesh S_1 and S_2. Then through the converging nozzle B air flows into the test channel C with cross section of rectangular form. Its upper and lower surfaces, which were constructed from plywood and coated with varnish, are parallel. The side

1) Th. v. Kármán: Ueber laminare und tnrbulente Reibung. Z. A. M. M. Bd. 1, 1921.

2) L. Prandtl: Ueber den Reibungswiderstand strömender Luft. Ergebnisse der Aerodyn. Versuchsanstalt zu Göttingen, 3. Lieferung.

3) E. Gruschwitz: Die turbulente Reibungsschicht in ebener Strömung bei Druckabfall und Druckanstieg. Ingenieur-Archiv Bd. 2, 1931, also Z. F. M. Nr. 11, 1932.

4) A. Buri: Eine Berechnungsgrundlage für die turbulente Grenzschicht bei beschleunigter und verzögerter Grundströmung. Zürich, 1931.

5) Fr. Dönch: Divergente und konvergente turbulente Strömungen mit kleinen Oeflunungswinkeln. Forsch.-Arb. Ing.-Wes. Heft 282, 1926.

6) J. Nikuradse: Untersuchungen über die Strömungen des Wasser in konvergenten und divergenten Kanälen. Forsch.-Arb. Ing.-Wes. Heft 289, 1929.

7) These experiments were carried out with the aid of Messrs. E. Simomura and T. Hirata.

Fig. 1.

Arrangements of the Experiment.

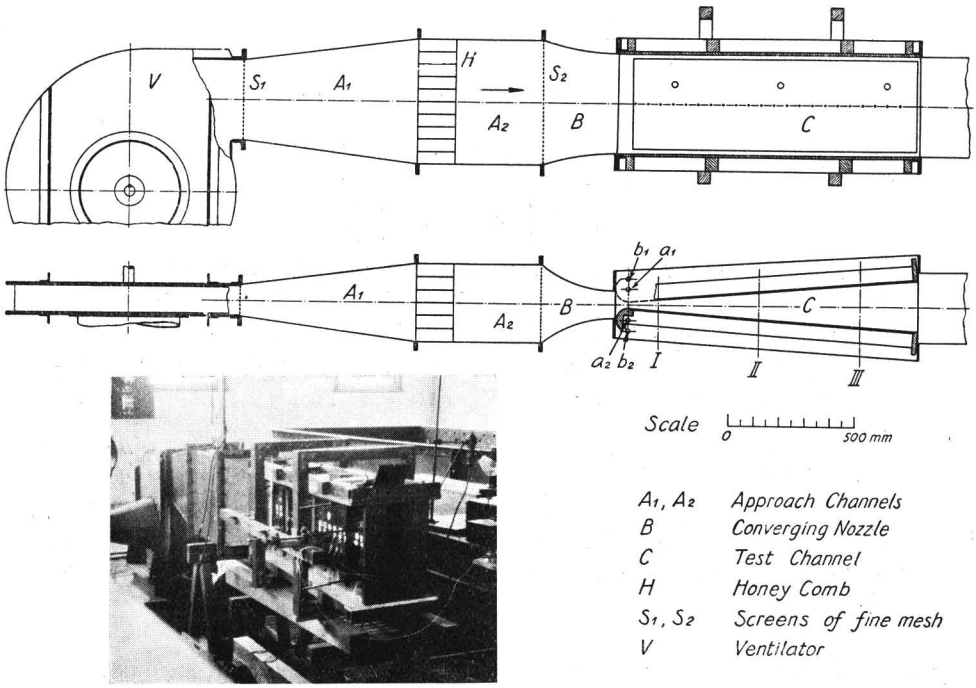

walls are covered with thick brass plates. They are bolted to the holes of a_1 and a_2 and rotate about these bolts so the diverging angle can be adjusted. By fastening the walls to the holes b_1 and b_2 instead of a_1 and a_2, the channel is made wider. There are several holes of 0.5 mm diameter on both side walls for the measurements of static pressure.

Fig. 2.

Velocity Distributions of Diverging Flow.

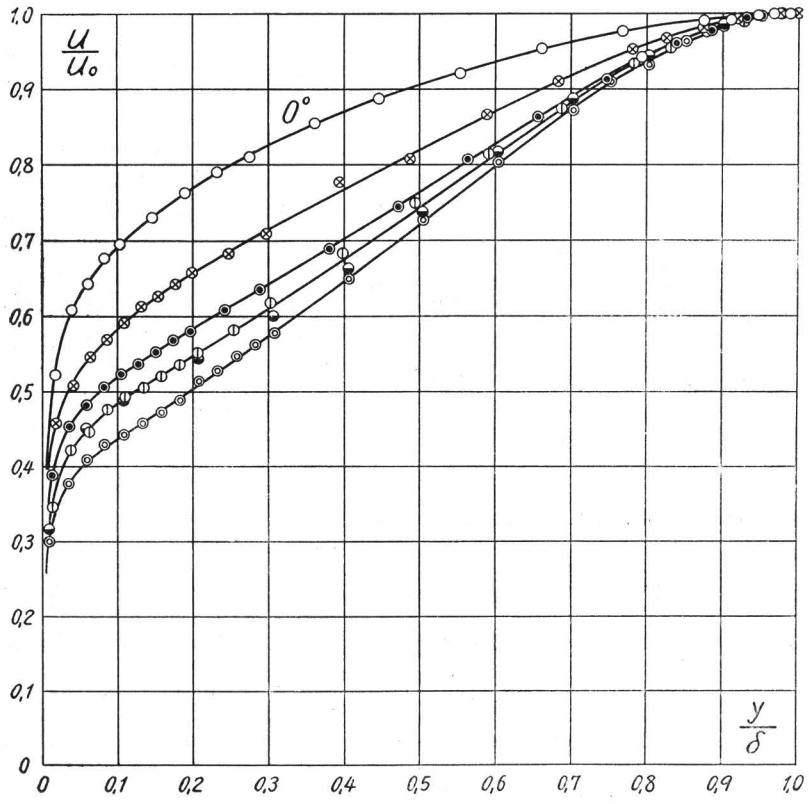

Velocity distributions are measured at sections I, II and III, mainly at the sections II and III. The Pitot-tubes for the measurements are made of copper drawn tubes of 1 mm outer diameter 0.5 mm inner diameter or 0.5 mm outer diameter 0.25 mm inner diameter. Pressure is measured by an inclined-tube type micromanometer using alcohol as its fluid and from the readings of this manometer, and readings of thermometer and barometerstand, the air velocities are calculated.

The measured velocity distributions at the middle height of the channel are shown in Fig. 2. When the diverging angle is small, the velocity distributions have almost symmetrical formes so they are plotted only on one side in dimensionless form, taking the maximum velocity as unity on the ordinate axis and the distance of the point of maximum velocity from the wall equal to one on the abscissa axis. The velocity distribution marked $0°$ in Fig. 2 is the one when the diverging angle is equal to zero or

the case of flow between parallel plates. Unfortunately owing to a lack of skill in manufacture, the surface of the brass plates are somewhat rough and not strictly flat, so the measured velocity distribution deviates from that measured in smooth pipes. The Reynolds' numbers of these tests lie between $3.4 \cdot 10^4$ and $8.8 \cdot 10^4$. Here the Reynolds' number is defined by the product of the mean velocity and breadth of the channel, divided by the coefficient of kinematic viscosity.

When the diverging angle becomes large, back flow takes place and the flow is no longer two-dimensional. The velocity distributions in such cases are shown in Fig. 3a, 20a and 20b in which small circles show the measured points. In these cases the velocity distrtbution losses its symmetrical nature so both sides were replotted again in the same manner as Fig. 2. Fig. 3b corresponds to the velocity distribution shown in Fig. 3a,

Fig. 3a.

Velocity Distribution of Diverging Flow.

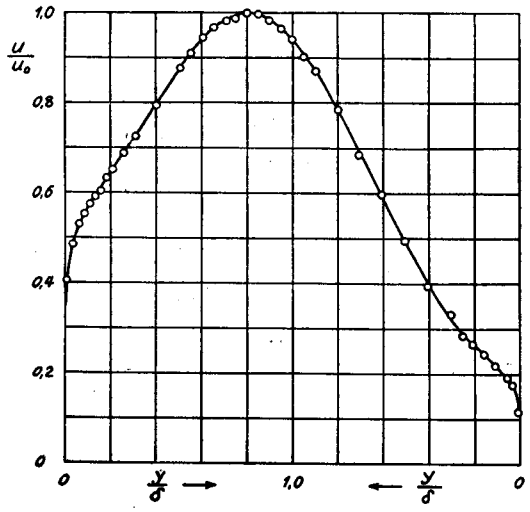

Fig. 3b.

Velocity Distributions of Diverging Flow.

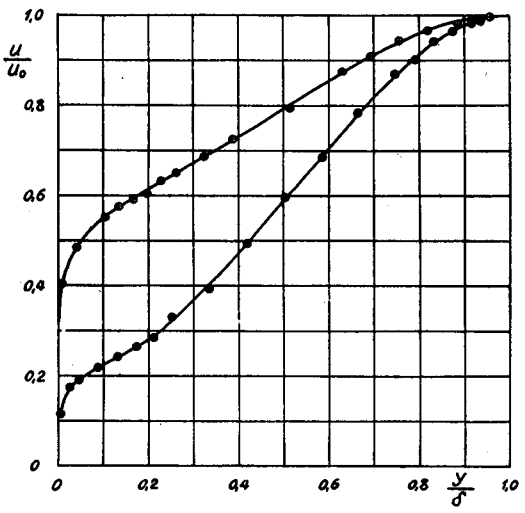

Fig. 4a.

Velocity Distributions of Diverging Flow.

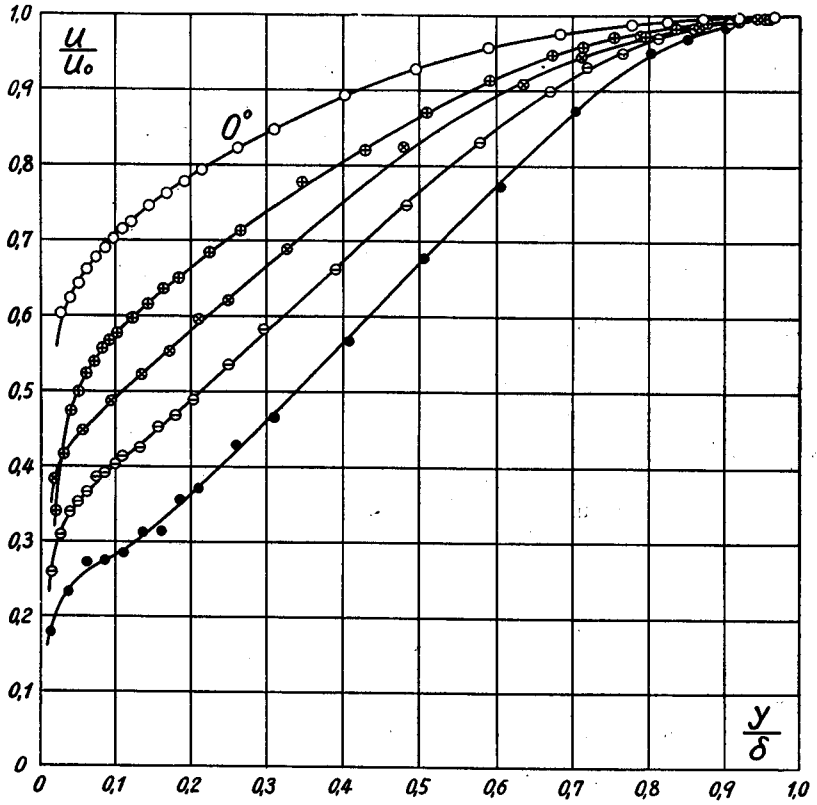

On the other hand if the breadth of the channel is made wide, the velocity distribution shows a section of uniform velocity at the center part of the flow forming turbulent boundary layers on both sides of the channel walls. In Fig. 4, some velocity distributions in the boundary layers are shown taking their thicknesses, which we may denote by the letter δ, as unity on the abscissa axis in quite the same way as Fig. 2. The curve marked $O°$ shows also the velocity distribution when the walls are parallel and 2δ becomes approximately equal to the breadth of the channel. The Reynolds' numbers of the boundary layers of these tests lie between $1.9 \cdot 10^4$ and $3.1 \cdot 10^4$, when it is defined as the product of the velocity just outside the boundary layer times its thickness, divided by the coefficient of kinematic viscosity.

Fig. 4b.

Velocity D'stributions of Diverging Flow.

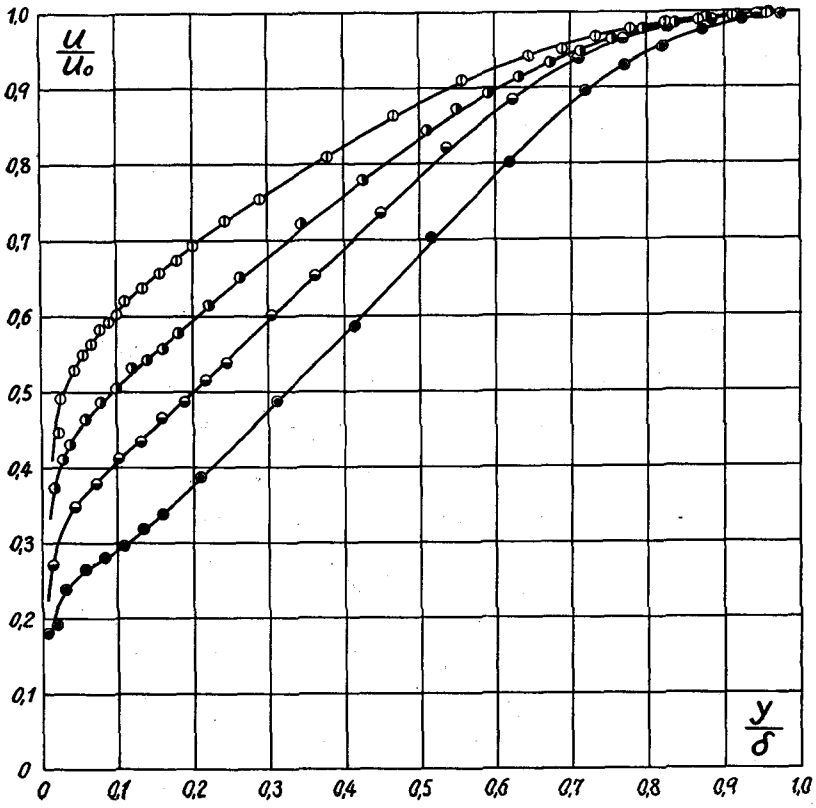

2. Approximate Expression of the Velocity Distributions with Single Parameter.

From the test results explained in the preceding section, an attempt to express these varying forms of velocity distributions by introducing a parameter was performed. In the following these are explained.

At first we express the velocity distribution in the parallel wall or along the flat plate by equation (1)

$$u=u_0 g\left(\frac{y}{\delta}\right), \quad \cdots\cdots(1)$$

where δ=thickness of the boundary layer or the distance of the maximum velocity from the wall surface,

u =velocity at distance y from the wall,

u_0=maximum velocity which occurs at $y=\delta$.

$g\left(\frac{y}{\delta}\right)$ is a function of $\frac{y}{\delta}$ satisfying $g(1)=1$. The form of it is well known from many experiments for both smooth and rough surfaces and also from theoretical investigation. For smooth surfaces the simplest form will be

$$g\left(\frac{y}{\delta}\right)=\left(\frac{y}{\delta}\right)^{\frac{1}{n}},$$

where n varies from 6 to 10 according the Reynolds' number.[8]

Then to express the velocity distributions for diverging flow, an equation of the following form is taken

$$u=u_0 g\left(\frac{y}{\delta}\right)\times \left\{m+(1-m)h\left(\frac{y}{\delta}\right)\right\}, \cdots(2)$$

where m is a parameter and mere number and $h\left(\frac{y}{\delta}\right)$ is a function of $\frac{y}{\delta}$ satisfying $h(1)=1$ and $h<1$ for $0<\frac{y}{\delta}<1$.

For the function $g\left(\frac{y}{\delta}\right)$, the velocity distribution of $O°$ was taken in the present case. To find $h\left(\frac{y}{\delta}\right)$, the ratio of a velocity distribution to that of $O°$ was first calculated. It gives

$$m+(1-m)\ h\left(\frac{y}{\delta}\right).$$

The values of calculated ratios are shown in Fig. 5 for the velocity distributions of Fig. 2 and 3b. From Fig. 5 the value of m for an individual case may be estimated, then h can be determined. But in reality, values of the ratios at $y=0$ are very ambiguous, so m was determined from the value at $\frac{y}{\delta}=0{,}1$ for convenience. To find h the value of $h(0{,}1)$ was assumed to be zero. Fig. 6 was obtained by calculating in this way for the measured points. Owing to the reduced accuracy of the experiments and the difficulties of measuring the turbulent flow, these calculated points scattered appreciably but practically they lie on one curve. In Fig. 7 and 8 some calculated results of the experiments by Dönch[9] and Nikuradse[10] are shown for comparison.

8) Equation (2) has no theoretical basis, so it must be corrected after an accurate theory for the turbulent boundary layer has been formulated. But for practical purpose, it is better to express the form of the velocity distribution as simply as possible. As one of the simplest, equation (2) was taken. It is therefore assumed that $h\left(\frac{y}{\delta}\right)$ is constant for all velocity distributions, but precisely, it seems to vary with m which must be investigated in the future, using more accurate methods and accurately finished channels. Further, it seems that $h(0)>0$ and there is a point of minimum for h between $\frac{y}{\delta}=0$ and $\frac{y}{\delta}=1.0$ but it is hard to obtain.

9) Dönch: loc. cit. footnote 5.

10) Nikuradse: loc. cit. footnote 6.

Fig. 5.

Ratios of the Velocities in Fig. 2.

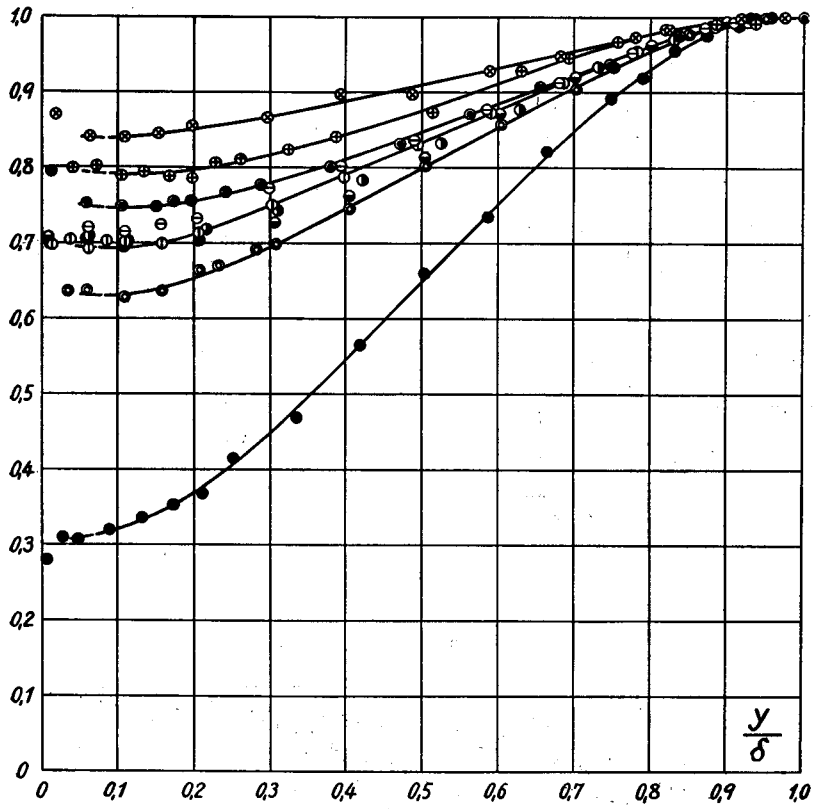

Fig. 6.

$h\left(\frac{y}{\delta}\right)$ for Fig. 2.

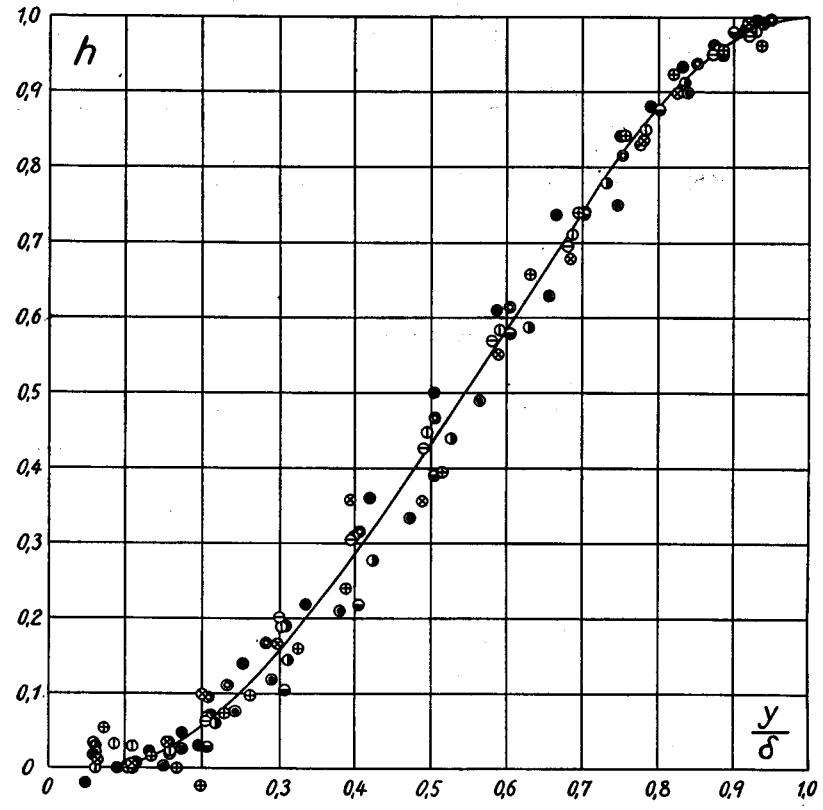

Fig. 7.

$h\left(\frac{y}{\delta}\right)$ of Dönch's Experiment.

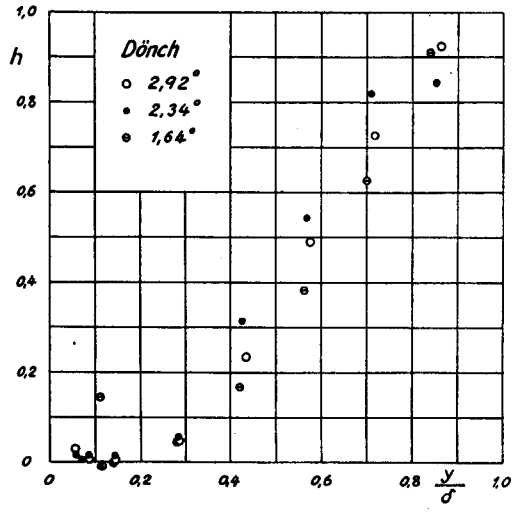

Fig. 8.

$h\left(\frac{y}{\delta}\right)$ of Nikuradse's Experiment.

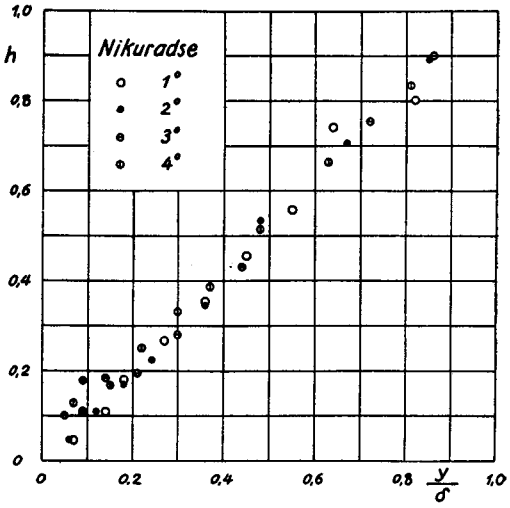

Fig. 9.

Ratios of the Velocities in Fig. 4.

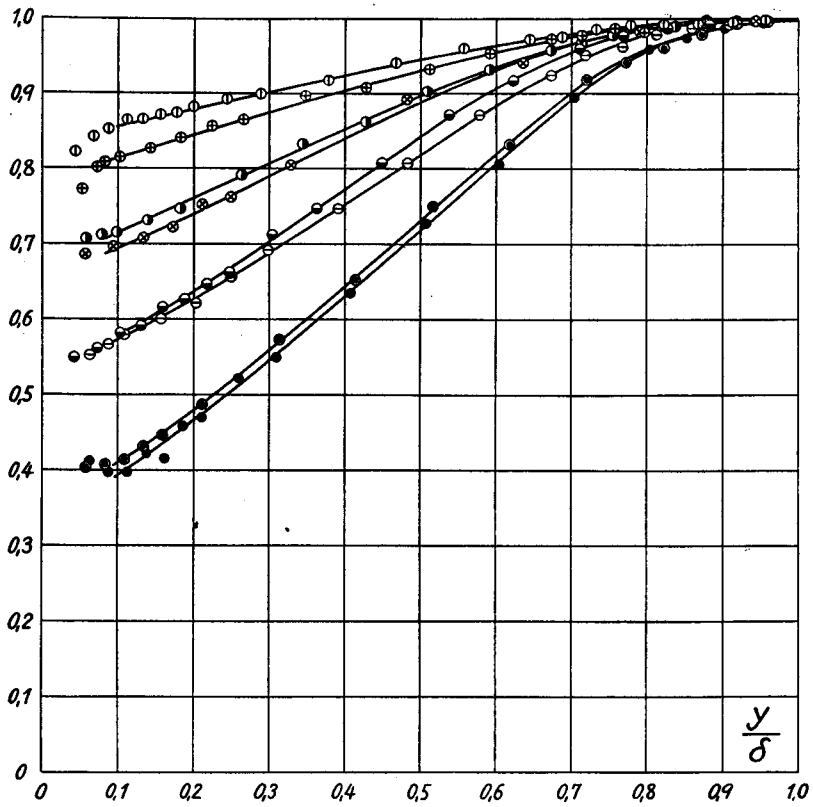

Our curve shown in Fig. 6 resembles exceedingly with the curve of the velocity distribution of a two-dimensional free jet measured by Förthmann.[11] But this may not be accidental because a free jet is the limiting case of diverging flow when the diverging angle becomes large. Also the flow in a diverging channel has more or less the nature of a free jet.

The same procedure was carried out for the velocity distributions of Fig. 4, shown in Fig. 9 and 10. In the previous case $h(0.1)\approx h(0)$ but in this case $h(0.1)>h(0)$, so at first it was assumed

11) E. Förthmann: Ueber turbulente Strahlausbreitung. Ingenieur-Archiv Bd. 5, 1934.

Fig. 10.

$h\left(\frac{y}{\delta}\right)$ for Fig. 4.

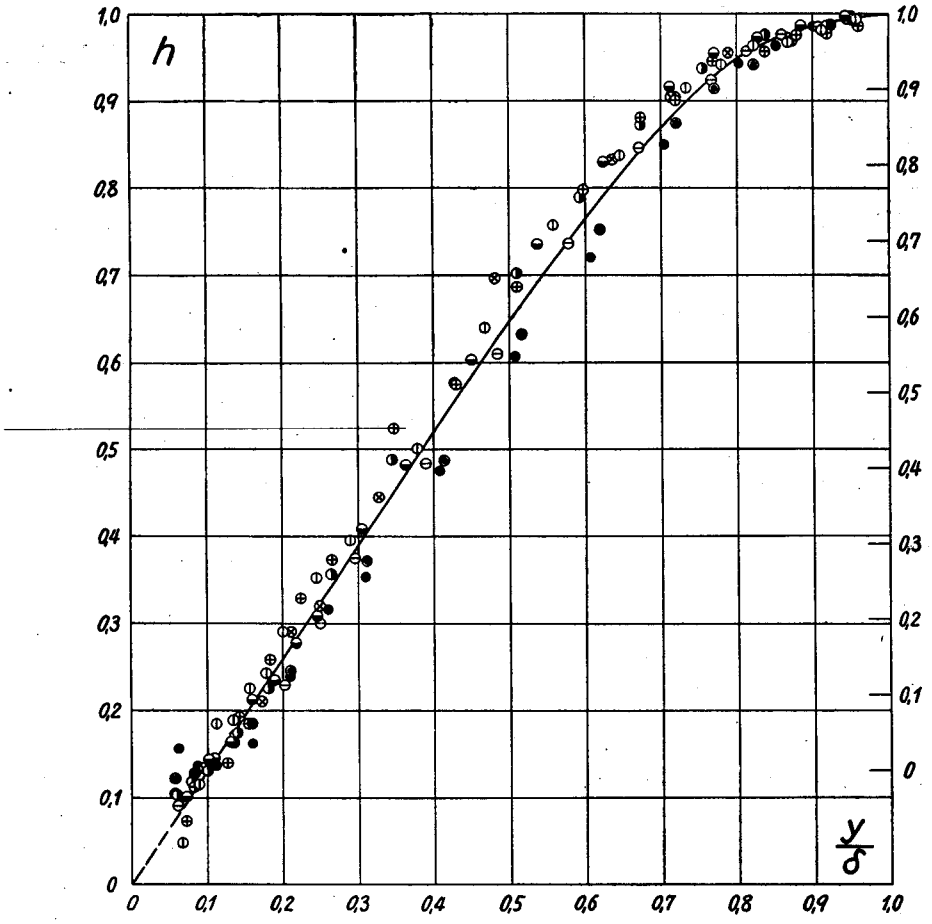

Fig. 11.

h-curve and Computed Velocity Distributions by Eq. (2). The Dotted Line is the Experimental Result of Nikuradse ($\alpha = 0°$).

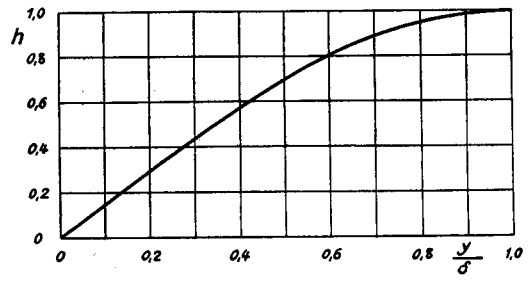

$h(0.1)=0$ and calculated points were plotted. From them the probable mean curve was drawn and extending this curve to the ordinate axis, the intersection was found. In Fig. 10, the scale of the ordinate axis is so changed that $h(0)=0$ and this scale is shown on the left hand side, while the old scale is shown on the right hand side of the diagram. The *h*-curve differs from that of Fig. 6. Also the probable *h*-curve deduced from

(Fig. 11 continued)

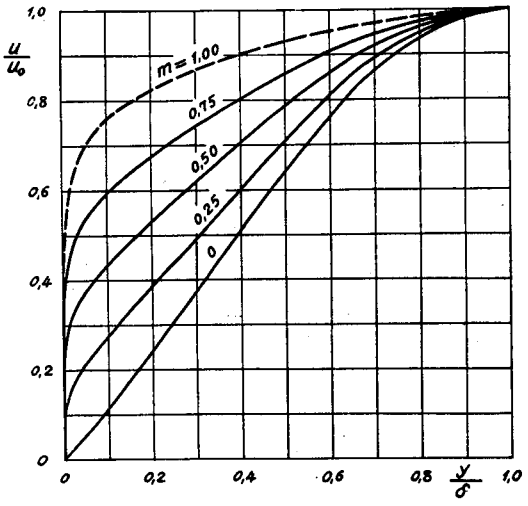

the experimental results of Gruschwitz[12] (test series 3) and some calculated forms of velocity distributions are shown in Fig. 11.

For the converging flow, some velocity distributions are shown in Fig. 12. The ratios of

12) Gruschwitz: loc. cit. footnote 3.

Fig. 12.

Velocity Distributions of Converging Flow.

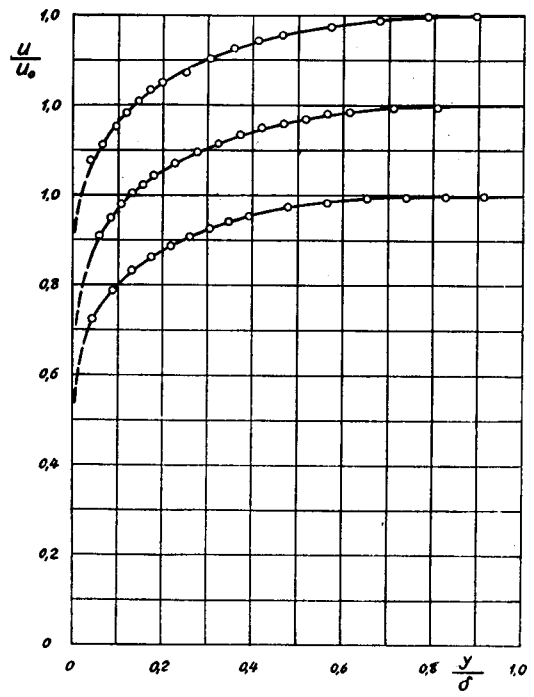

Fig. 13.

Ratios of Velocities in Fig. 12 and other Experiments.

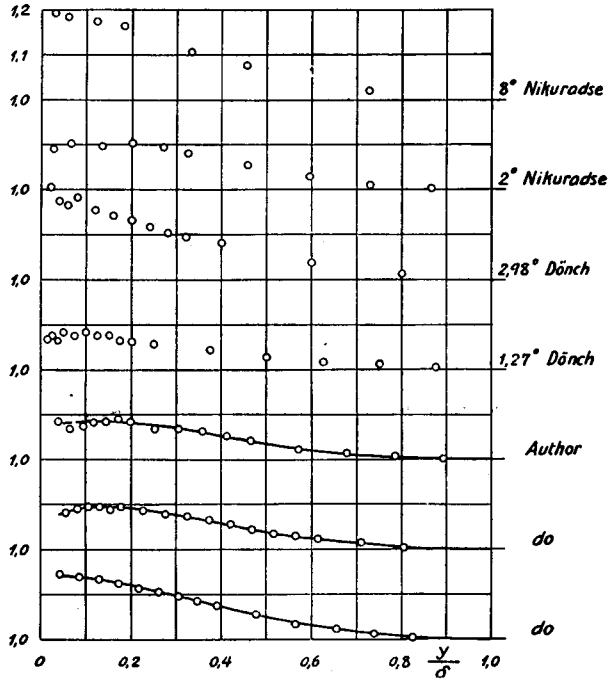

velocities with that of $0°$ are shown in Fig. 13 with some results of Dönch and Nikuradse. From Fig. 13 it may be concluded that the ratios can be also expressed in the form of

$$m+(1-m)\,h\left(\frac{y}{\delta}\right),$$

where $m>1$.

3. Analytical Research of the Turbulent Flow in Diverging Channels.

Before making the experiments described above, the author had attempted to express the velocity distributions by a simple formula and thence he got a result on the break-away of flow in diverging channels. To examine whether such a result is plausible or not, was one of the objects of the present experiment, though it failed to give a definite conclusion, since the flow is already not two-dimensional when the break-away or back flow takes place. The calculation carried out then and the results of the experiment are as follows.

We considered the turbulent two-dimensional flow of an incompressible fluid in diverging channels as shown in Fig. 14. We take the channel

Fig. 14.

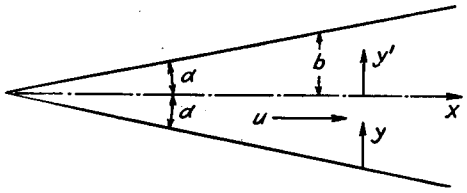

axis as x and denote the half breadth of the channel by b, the diverging angle by α, then if the angle is small we can say $b=\alpha x$. We denote the distance from the wall by y and let $y'=b-y$ and express the velocity distribution in the following form;

$$u=u_0\left(\frac{y}{b}\right)^{\frac{1}{n}}\left\{m+m_1\left(\frac{y}{b}\right)+m_2\left(\frac{y}{b}\right)^2+\cdots\right\},\quad\cdots(3)$$

where u is the velocity at distance y and u_0 is the velocity at the center, i.e. at $y=b$. Considering the velocity distribution is symmetrical with respect to the x-axis, and m, m_1 ..... are mere numbers.

For the convenience of calculation, we assume $n=7$ and

$$u=u_0\left(\frac{y}{b}\right)^{\frac{1}{7}}\left\{m+m_1\left(\frac{y}{b}\right)+m_2\left(\frac{y}{b}\right)^8\right\},\quad\cdots\cdots(4)^{13)}$$

where m_1 and m_2 are determined by the conditions

$$u=u_0 \quad\text{and}\quad \frac{du}{dy}=0 \quad\text{at}\quad y=b.$$

Some of so computed forms are shown in Fig. 15.

Let

$$\psi=\frac{1}{u_0 b}\int_0^b u\,dy$$

13) This part was read before the meeting of the Kikai-Gakkwai-Kwansai-Sibu in March, 1932. Now it seems better to take the velocity distribution given by equation (2), but there is no change in the principle of calculation, so it left unaltered.

Fig. 15.

Assumed Velocity Distributions by Eq. (4).

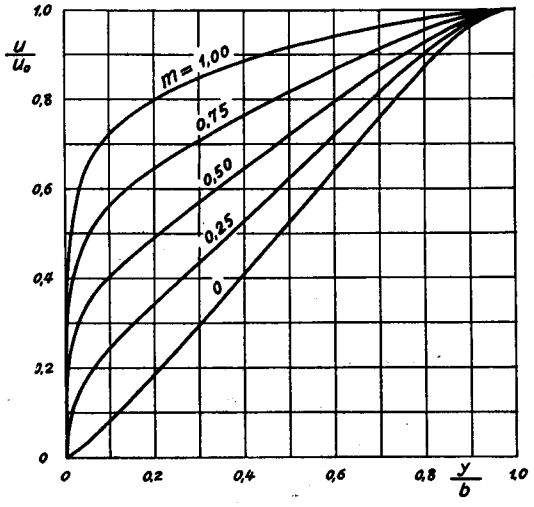

and the value of $R=\frac{2u_0b\psi}{\nu}$ was taken as the Reynolds' number of the flow, ν being the coefficient of kinematic viscosity.

Now let the pressure of fluid to be denoted by p, the shearing stress at y by τ and the density of fluid by ρ which is a constant value. Then in the case of steady flow, we have

$$\frac{\rho}{2}\int_0^{y'}\frac{du^2}{dx}dy'=-y'\frac{dp}{dx}-\tau, \quad \cdots\cdots(5)$$

assuming that a is small and p is constant over the cross section perpendicular to the x-axis. Hence if we assume the velocity distribution changes along the x-axis but "affin", then

$$\frac{dp}{dx}=\rho\frac{\varphi u_0^2}{x}-\frac{\tau_0}{b}, \quad \cdots\cdots(6)$$

where

$$\varphi=\frac{1}{u_0^2b}\int_0^b u^2dy,$$

and τ_0 is the shearing stress at the wall surface and it is assumed as follows;

$$\tau_0=0.0225\ \rho m^2u_0^2\left\{\frac{\nu}{mu_0b}\right\}^{\frac{1}{4}},$$

or

$$\frac{\tau_0}{\rho u_0^2}=0.02676\left(\frac{1}{R}\right)^{\frac{1}{4}}m^{\frac{7}{4}}\psi^{\frac{1}{4}}. \quad \cdots\cdots(7)$$

From equations (5) and (6) we get

$$\frac{\tau}{\rho u_0^2}=-\frac{y'}{b}\left\{a\varphi-\frac{\tau_0}{\rho u_0^2}\right\}+a\int_0^{\frac{y'}{b}}\left(\frac{u}{u_0}\right)^2d\left(\frac{y'}{b}\right). \quad \cdots\cdots(8)$$

Following Prandtl we express τ by using the length l, i.e. the so-called "Mischungsweg"[14] or

$$\tau=\rho l^2\left|\frac{du}{dy}\right|\frac{du}{dy} \quad \cdots\cdots(9)$$

The value of l varies from place to place. The theoretical value of l is not yet known except as deduced by Kármán[15] in the case of the flow between two parallel plates. It may be assumed therefore after the experiments of Nikuradse[16] as follows; l is proportional to x and the value of l/b at the center part of the channel is approximately independent of a. Further we assume $m=1$ corresponds to $a=0$ and by this case $l/b=0.1235$ at $y/b=0.8$, when $R=2.86\cdot10^4$[17].

Equating the value of l/b at $y/b=0.8$ to 0.1235 when $R=2.86\cdot10^4$ for all angles of a, we get the following relation

$$a=\frac{0.1235^2\left\{d\left(\frac{u}{u_0}\right)\Big/d\left(\frac{y}{b}\right)\right\}^2_{y/b=0.8}-0.2\frac{\tau_0}{\rho u_0^2}}{\int_0^{0.2}\left(\frac{u}{u_0}\right)^2d\left(\frac{y'}{b}\right)-0.2\varphi} \quad \cdots\cdots(10)$$

The computed relation between m and $aR^{\frac{1}{4}}$ is shown in Fig. 16 with the measured values of Nikuradse. The distributions of l are shown in Fig. 17.

Fig. 16.

Relation between Parameter m and $aR^{\frac{1}{4}}$.

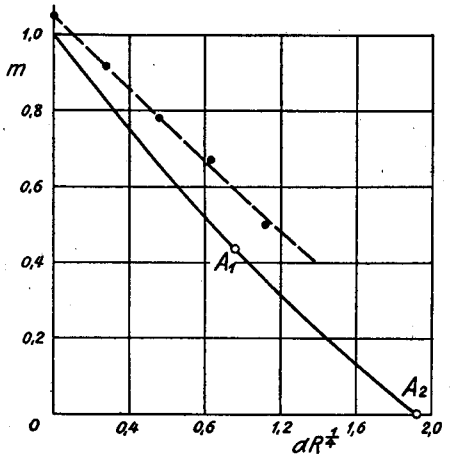

• Nikuradse (estimated)

In this way we find $m=0$ corresponds to $aR^{\frac{1}{4}}=1.919$ or

$$a=8.46^0 \quad \text{when} \quad R=2.86\cdot10^4.$$

At and above this angle the flow breaks away from the channel wall on both sides.

Then a question arises whether for a smaller

14) For example, see Handbuch der Experimentalphysik, Bd. 4, Teil 1, page 309.

15) Th. v. Kármán: Mechanische Aehnlichkeit und Turbulenz. Proceedings of the 3rd International Congress for Applied Mechanics, Vol. 1.

16) Nikuradse: loc. cit. footnote 6.

17) It is impossible to find l/b at $y/b=1.0$ in this calculation.

Fig. 17.

Computed l-distributions.

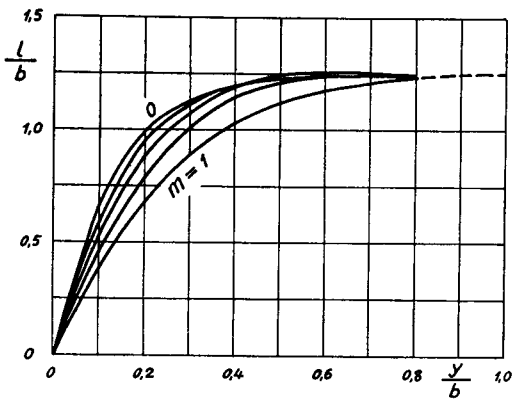

angle, back flow takes place or not; in other words whether back flow on one side only of the channel wall is possible or not. After trial calculation, it was found that when $aR^{\frac{1}{4}}=0.958$, it is possible that $m=0$ on one side only while $m\approx 0.77$ on the other side of the wall giving an unsymmetrical velocity distribution but with the same value of l at the center part. The velocity and l distributions in this case are shown in Fig. 18.

Fig. 18.

Computed Velocity and l-distributions for Unsymmetrical Break-away.

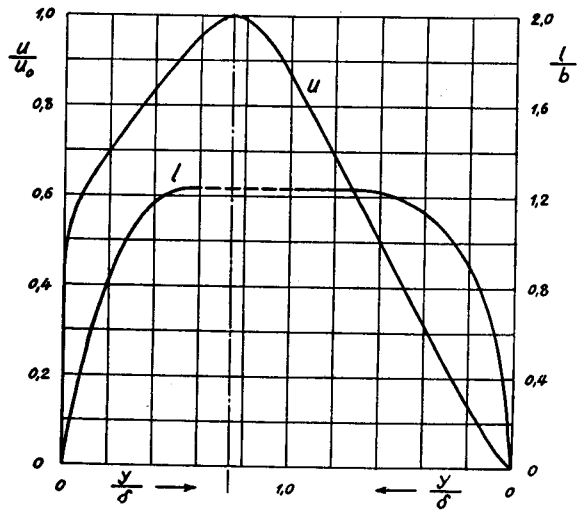

If the angle is larger than the above, flow may perhaps break away on one side when the symmetry of flow is disturbed. We may term this type of flow unsymmetrical break-away (its limit being indicated by point A_1 in Fig. 18) against break-away of a symmetrical form (indicated by point A_2 in the same figure).

The ratio of the angles of these back flow is

$$\frac{\theta_{\text{unsymmetrical break-away}}}{\theta_{\text{symmetrical break-away}}}=0.499\approx 0.5,$$

and the range of $aR^{\frac{1}{4}}$ is divided into three parts, viz.

$aR^{\frac{1}{4}}<0.958$ no back flow,

$0.958<aR^{\frac{1}{4}}<1.919$ back flow may take place on one side,

$aR^{\frac{1}{4}}>1.919$ back flow on both sides.

They are shown diagramatically in Fig. 19.

Fig. 19.

Schematic Diagrams for the Relation between Diverging Angle and Break-away.

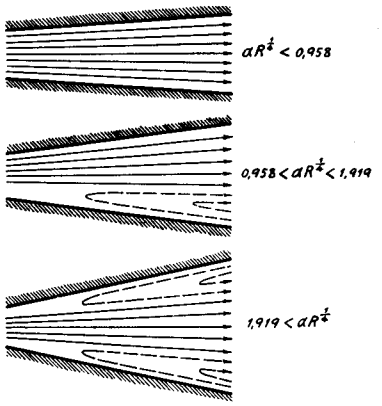

In Fig. 20a and 20b some results of measurements of unsymmetrical break-away are shown compared with the computed result. Fig. 20c is the corresponding symmetrical case. But they are all measured at the middle height of the channel. Now in these cases the flow is no longer two-dimensional, so the form of velocity distribution may vary considerably with the height, and the above measurements will only exist in that section and is of quite different form at another height. So the above computation is not perfectly demonstrated but we can conclude that the velocity distribution with m less than approximately 0.4 is

Fig. 20a.

Computed and Experimental Results.

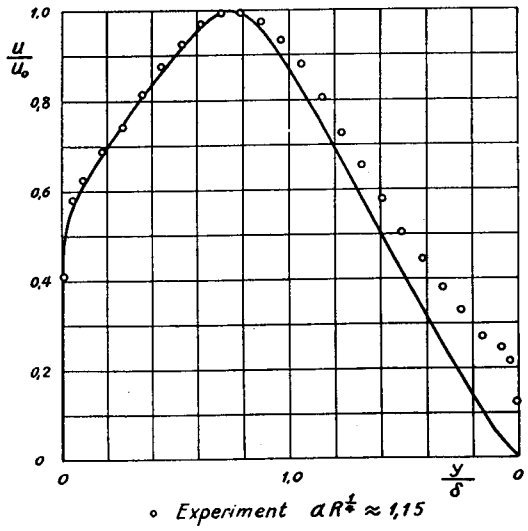

Fig. 20b.
Ditto.

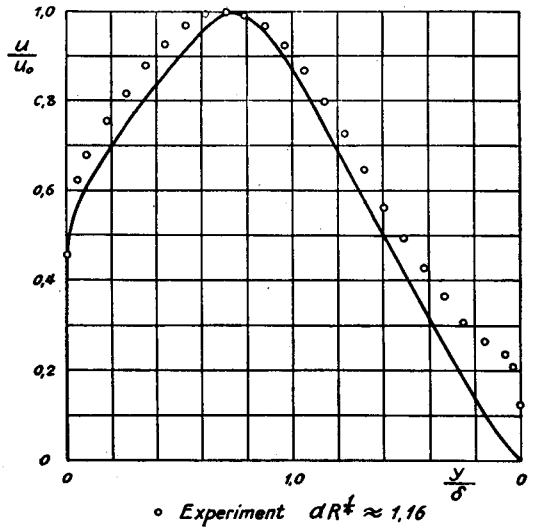

Fig. 20c.
Ditto.

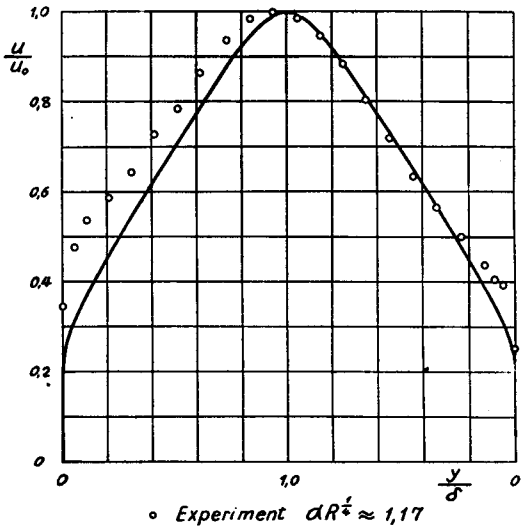

not stable and apt to break away; which has been also ascertained by Nikuradse's experiment.

4. Some Examples of Flow along the Surface of Revolution.

The typical forms of velocity distributions in the turbulent boundary layers are shown in Fig. 21a; one, when there is no pressure change, the other two when pressure rises or falls along the direction of flow. The corresponding shearing stress distributions, according Buri, are shown in Fig. 21b taking the shearing stress τ divided by the shearing stress τ_0 at the surface of the wall as the ordinate axis and y/δ as the abscissa axis.

Now we will consider a small portion of fluid

Fig. 21.
Approximate Velocity and Shearing Stress Distributions.

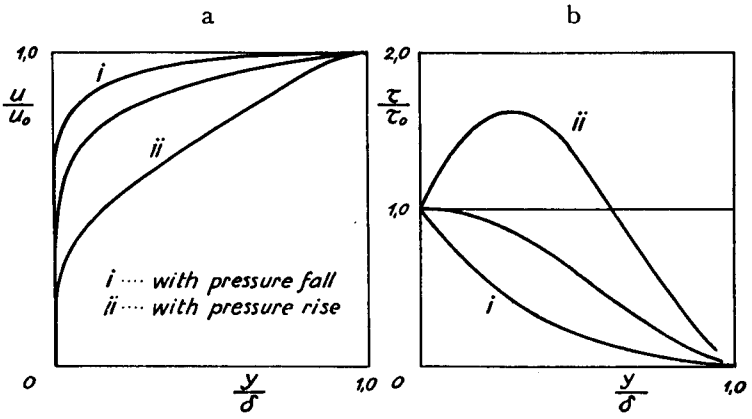

at the surface of the wall, a very short distance from the surface, and denote the y-component of velocity by v, then

$$u\frac{\partial u}{\partial x}+v\frac{\partial u}{\partial y}=-\frac{1}{\rho}\frac{dp}{dx}+\frac{1}{\rho}\frac{\partial \tau}{\partial y}.$$

And as a rough approximation we assume that the second term of the left hand side is small compared with the first term and can be neglected, then

$$u\frac{\partial u}{\partial x}=-\frac{1}{\rho}\frac{dp}{dx}+\frac{1}{\rho}\frac{\partial \tau}{\partial y}. \quad \ldots\ldots\ldots\ldots\ldots (11)$$

In the case of laminar flow, $u=0$ at the wall surface and

$$\frac{1}{\rho}\frac{dp}{dx}=\nu\frac{\partial^2 u}{\partial y^2}.$$

In the case of turbulent flow, $u\neq 0$ in the close neighbourhood of the wall, and we denote this velocity by

$$u_{\text{wall}}=nu_0,$$

where u_0 is the velocity just outside the boundary layer and n is a mere number less than one.

Then by the relation

$$u_0\frac{du_0}{dx}=-\frac{1}{\rho}\frac{dp}{dx},$$

we get

$$\frac{dn}{dx}=-\frac{(1-n^2)}{2n}\frac{1}{q}\frac{dp}{dx}+\frac{1}{n\delta}\frac{\delta}{\rho u_0^2}\left(\frac{\partial \tau}{\partial y}\right)_0, \quad \ldots (12)$$

where $\left(\frac{\partial \tau}{\partial y}\right)_0$ is the value of $\frac{\partial \tau}{\partial y}$ at the wall and $q=\frac{\rho}{2}u_0^2$. Now n may be expressed by introducing the above mentioned parameter m viz.

$$n=n_0 m$$

where n_0 is the value of n, when $m=1$.
Putting this into equation (12) we get

18) Buri: loc. cit. footnote 4.

$$\frac{dm}{dx}=-\frac{(1-n_0^2m^2)}{2mn_0^2}\frac{1}{q}\frac{dp}{dx}$$
$$+\frac{1}{mn_0^2\delta}\frac{\delta}{\rho u_0^2}\left(\frac{\partial\tau}{\partial y}\right)_0 \quad \text{.....(13)}$$

and according to Fig. 21b

$\left(\frac{\partial\tau}{\partial y}\right)=0$ for $\frac{dp}{dx}=0$ or flow along the flat plate placed edgewise to the stream. We may denote the value of m in this case by m_0,

$\left(\frac{\partial\tau}{\partial y}\right)_0>0$ for $\frac{dp}{dx}>0$ or $m<m_0$,

$\left(\frac{\partial\tau}{\partial y}\right)_0<0$ for $\frac{dp}{dx}<0$ or $m>m_0$.

The above equation (13) is deduced by a very simple consideration but it will be possible to express the rate of change of m by generalizing this equation i.e.

$$\frac{dm}{dx}=a(m)\frac{1}{q}\frac{dp}{dx}+\frac{b(m)}{\delta}, \quad \text{.....(14)}$$

where $a(m)$ and $b(m)$[19] are functions of m but yet unknown.

To determine these functions we make use of the empirical formula of Gruschwitz[20] viz.

$$\frac{\vartheta}{q}\frac{dg_1}{dx}=0.00894\eta-0.00461,$$

where

$$\vartheta=\int_0^\delta\frac{(u_0-u)u}{u_0}dy,$$
$$\eta=1-\left(\frac{u_1}{u_0}\right)^2,$$
$$g_1=p+\frac{\rho}{2}u_1^2,$$

u_1 being the velocity at $y=\vartheta$.

From this formula and the h-curve as shown in Fig. 11, we can compute the values of $a(m)$ and $b(m)$. The so computed results are shown in Fig. 22.

The validity of Gruschwitz's formula for every case is not yet confirmed but was proved recently by J. Stüper[21] in flight tests. Here, in the following lines, application of equation (14) to the surface of revolution may be mentioned.

In the case of converging flow in a conical tube with circular cross section, the velocity distribution at a cross section will show a region of uniform velocity at the center and the remaining parts near the wall surface form the boundary layers. In such a case the form of velocity distribution in the boundary layer is maintained almost

Fig. 22.
$a(m)$ and $b(m)$.

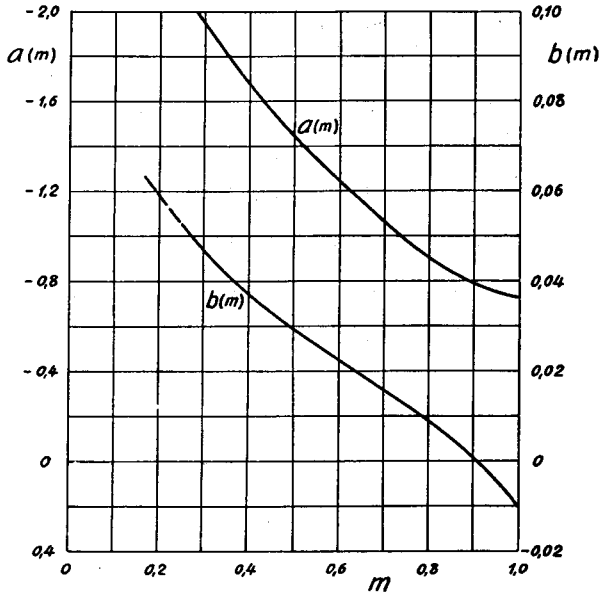

constant as indicated by the experimental result shown in Fig. 12. The ratio of the boundary layer thickness δ to the radius of the tube r_0 varies along the tube axis, which we denote as the x-axis. As a velocity distribution formula the following proves very useful,

$$u=u_0\left(\frac{y}{\delta}\right)^{\frac{1}{7}}\left(\frac{8}{7}-\frac{1}{7}\frac{y}{\delta}\right).$$

The equation of momentum, of continuity and Bernoulli's equation are as follows;

$$\left.\begin{aligned}\rho\frac{d}{dx}\int_0^{r_0}2\pi u^2rdr&=-\pi r_0^2\frac{dp}{dx}-2\pi r_0\tau_0,\\ \int_0^{r_0}2\pi urdr&=\text{const.},\\ u_0\frac{du_0}{dx}&=-\frac{1}{\rho}\frac{dp}{dx},\end{aligned}\right\}\text{.....(15)}$$

where u is the velocity at distance r from tube center and

$$u=u_0 \quad \text{for} \quad r<r_0-\delta.$$

From them we can determine the variation of δ with x. An example of such a calculation was carried out for a very smooth Venturi-tube of standard form. The computed coefficient of discharge from this example is plotted in full line against $\log_{10}\frac{u_md}{\nu}$ in Fig. 23, where u_m is the mean speed of fluid at the throat and d is the diameter of the throat. Laminar flow, assuming the velocity distribution in the boundary layer to be a parabola, is shown in the dotted line, while

19) $b(m)$ may not be only the function of m but Reynolds' number etc.
20) Gruschwitz: loc. cit. footnote 3.
21) J. Stüper: Untersuchung von Reibungsschichten am fliegenden Flugzeug. Luftfahrt-Forschung Bd. 11, Nr. 1, 1934.

Fig. 23.

Computed and Actual Coefficients of Discharge of the Venturi-tube.

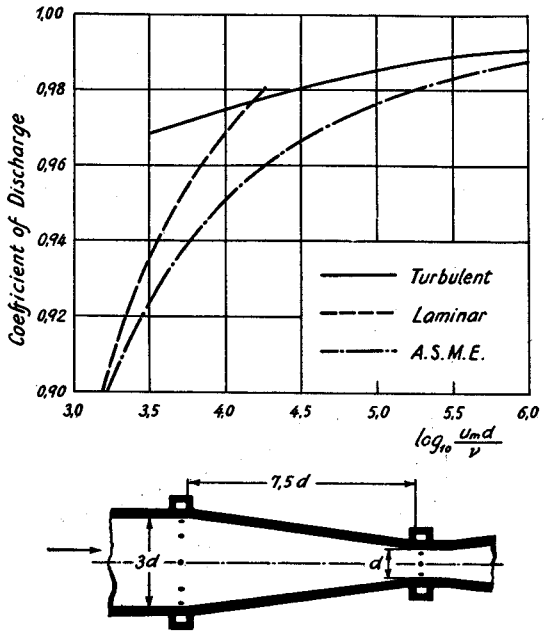

the mean curve given by A. S. M. E.[22] for Venturi-tubes in practical use is shown in chain line.

Next we take the problem of the turbulent boundary layer of an airship hull with its center line in the direction of flow. As an example, computation in the case of 1/40-scale model of the airship "Akron" was carried out and compared with the experimental results of H. Freeman.[23]

The equation of the boundary layer is

$$\frac{d}{dx}\int_0^\delta u^2 r\,dy - v_0\frac{d}{dx}\int_0^\delta u r\,dy = -\left(r_0\delta + \frac{\delta^2\cos\alpha}{2}\right)\frac{1}{\rho}\frac{dp}{dx} - \frac{r_0\tau_0}{\rho}, \quad (16)$$

where $\tau_0 = 0.0225\,\rho u_0^2 n^2\left(\frac{\nu}{m u_0 \delta}\right)^{\frac{1}{4}}$,

r_0 = radius of the hull,

u = velocity at distance y from the wall or distance r from the center line of the hull,

α = inclination of the tangent plane to the surface with the center line of the hull,

x = distance measured along the surface of the hull in the direction of flow.

Solving this equation with equation (14) we get the variation of δ and m. Calculation was carried out for the after-portion of the hull, from the measuring station No. 7 of Freeman's experiment. At this station, we assumed $\delta = 5.75$ cm and $m = 0.92$. The assumed velocity distribution is shown on the top of Fig. 24 which agrees with

Fig. 24.

Measured and Computed Velocity Distributions.

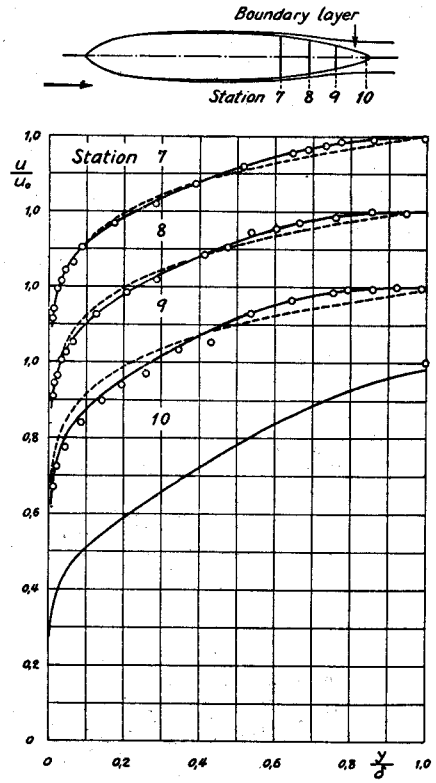

the experiment. Then velocity distributions at the stations 8, 9 and 10 were calculated and are shown in full lines in the same figure, the abscissa axis being shifted to avoid confusion. In this figure the dotted lines show computed results by the formula proposed by C. B. Millikan, taken from Freeman's paper, while the measured points are indicated by small circles. We find that we can get closer agreement with the experiment if we take the change of parameter m into account.

5. Relation between the Reynolds' Number and the Maximum Lift Coefficient of Aerofoil.

Generally the maximum lift coefficient of aerofoil varies with Reynolds' number. Kármán[24] has explained this point theoretically considering the transition of the laminar boundary layer to the

22) Fluid Meter, Their Theory and Application. A. S. M. E. Research Publication, 3rd Edition. E. Ower: Measurement of Air Flow. page 93.

23) H. Freeman: Measurements of Flow in the Boundary Layer of a 1/40-scale model of the U. S. Airship "Akron". N. A. C. A. Report No. 430, 1932.

24) Th. v. Kármán and C. B. Millikan: The Use of the Wind Tunnel in Connection with Aircraft-Design Problems. Transactions of A. S. M. E. March, 1934.

turbulent layer. But this only revealed the nature of the relation at rather low Reynolds' number. Gruschwitz[25] has also made qualitative explanation but over a wide range of the number. In this section, very rough and approximate considerations are made on the same subject by the aid of equation (14).

To make consideration easier we take two extreme cases, the one of thin aerofoil with small camber and the other of thick aerofoil with rounded nose, or thin aerofoil but with large camber. First we consider the former.

In Fig. 25, diagrams of the break-away of flow are shown. When the Reynolds' number is low the bonndary layer is laminar and breaks away from a point near the leading edge as shown in Fig. 25a. Increasing Reynolds' number, the

Fig. 25.

Diagrams of Flows about a Thin Aerofoil Section near c_z max.

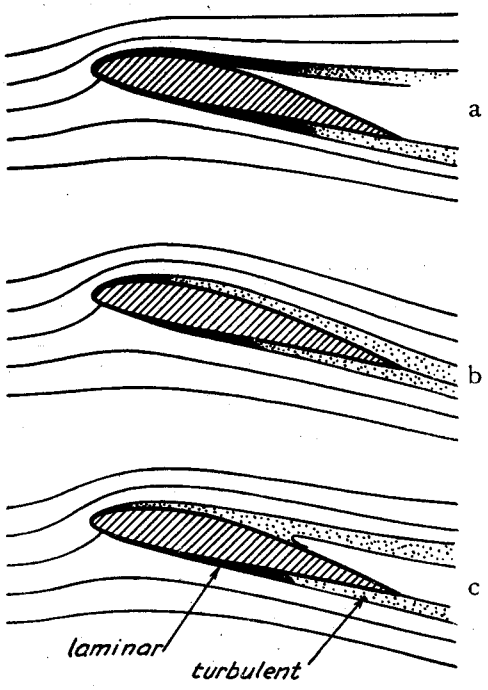

laminar boundary layer becomes turbulent before it breaks away, then the layer leans to the surface and no break-away occurs, hence the aerofoil is not yet burbled-Fig. 25b. But if the lift coefficient becomes large or the incidence angle becomes large, the turbulent boundary layer breaks away and the aerofoil is burbled-Fig. 25c.

The available result of systematic experiments on thin aerofoil at various Reynolds' number is that of N. A. C. A. 2412 section carried out at Pasadena[26]. Instead of this section, we take, for simplicity of calculation, the Joukowski section (Göttingen Nr. 541) which resembles the above mentioned aerofoil. Then in this case, velocities over the surface of aerofoil can be easily calculated by the theory of the potential flow, an example of which is shown in Fig. 26a. The abscissa is the arc length x over the upper surface of the

Fig. 26.

Computed Values of v_0^2, $\frac{1}{v_0^2}\frac{dv_0^2}{dx}$ and δ over the Upper Surface of the Aerofoil at $c_z \approx 1.17$.

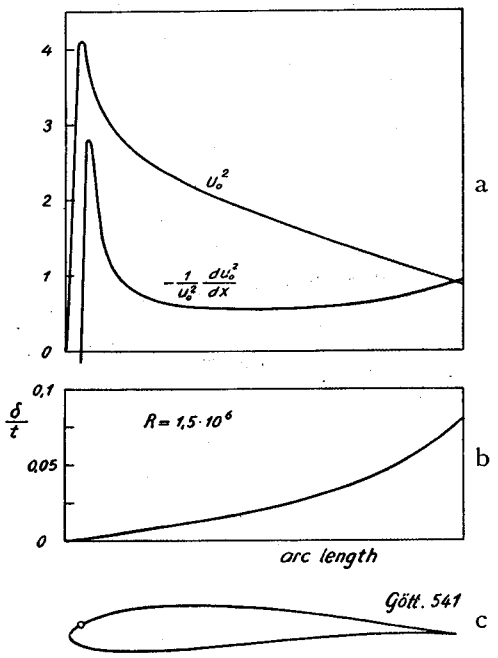

aerofoil, measured from the front stagnation point; the ordinate is the square of velocity when the lift coefficient is equal to about 1.17, and the velocity far from the aerofoil is taken as unity. The curve of the square of the velocity may be considered as the pressure distribution curve, only the length of the ordinate and its sign should be changed, others remaining the same. The most characteristic property of this curve is that at the nose, near the leading edge, there exists a heavy pressure rise. So at this part the laminar boundary layer, continued from the front stagnation point, possibly breaks away from the surface of the aerofoil. Or if not, it changes into the turbulent boundary layer according to the magnitude of Reynolds' number. For the case of break-away of laminar boundary layer, explanation has already been given by Kármán. We may consider the latter case. In this case it is permitted to assume that the boundary layer is already turbulent from the front stagnation point, this assumption being made for the convenience of calculation.

As a rough approximation, we integrate equa-

25) Gruschwitz: loc. cit. footnote 3.

26) Th. v. Kármán and C. B. Millikan: loc. cit. footnote 24.

tion (14) term by term from the point where the laminar boundary layer changes to turbulent, which is marked by the small circle in Fig. 26c in our case, then

$$\int_{\text{Transition point}}^{\text{Trailing edge}} dm = -\int \frac{a}{u_0^2} du_0^2 + \int \frac{b}{\delta} dx.$$

We write the right hand side in the following form,

$$\int dm = -a_0 \int \frac{du_0^2}{u_0^2} + b_0 \int \frac{dx}{\delta}, \quad \cdots\cdots(17)$$

where we take as a_0 and b_0 the mean values of a and b. And moreover we assume for convenience that the maximum lift coefficient had been reached when, at the trailing edge, m becomes zero. So for the maximum lift coefficient the left hand side has a negative definite value.

The first term on the right hand side chiefly depends upon the lift coefficient c_z, and the second term may also depend upon c_z but is greatly influenced by the Reynolds' number. In our case the first integral can be expressed approximately as a linear function of c_z i.e.,

$$-\int \frac{du_0^2}{u_0^2} = 0.906\, c_z + 0.334.$$

The boundary layer thickness δ was approximately computed taking the velocity distribution in the following form

$$u = u_0 \left(\frac{y}{\delta}\right)^{\frac{1}{7}},$$

by the formula proposed first by M. Ono[27] and later by H. Müller, an example of which is shown in Fig. 26b. The thickness δ is proportional to $R^{\frac{1}{5}}$ as in the case of flat plate placed edgewise to the stream, where

$$R = \frac{wt}{\nu},$$

w is air velocity and t is the length of chord.

After several computations the second integral can be expressed approximately by a linear function of c_z and proportional to $R^{\frac{1}{5}}$ i.e.,

$$\int \frac{dx}{\delta} = R^{\frac{1}{5}}(8.08 - 3.14\, c_z).$$

Moreover an example of calculation was carried out taking

$$R = 1.5 \cdot 10^6, \quad c_z = 1.174,$$

and at these values m is nearly zero at the trailing edge. Estimating the mean values of a_0 and b_0 from this example, equation (17) can be written in the following form

$$c_{z\,\max} + 0.0297\, c_{z\,\max} R^{\frac{1}{5}} - 0.0766\, R^{\frac{1}{5}} = 0.458 \quad \cdots\cdots(18)$$

The value of the integral on the left hand side of equation (17) was so controlled that $c_{z\,\max} = 1.174$ at $R = 1.5 \cdot 10^6$. This equation (18) is shown in full line in Fig. 27 while the broken line shows the following equation :

Fig. 27.

Relation between $c_{z\,\max}$ and R.
Small Circles show the Experimental Results at Göttingen.

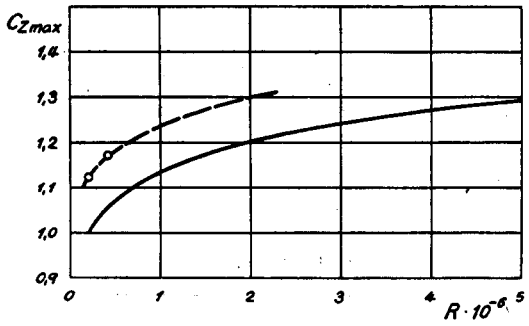

$$c_{z\,\max} + 0.0297\, c_{z\,\max} R^{\frac{1}{5}} - 0.0766\, R^{\frac{1}{5}} = 0.606,$$

by which the above mentioned constant was so changed that $c_{z\,\max} = 1.172$ at $R = 0.42 \cdot 10^6$ which values correspond to the test result of Göttingen.[28]

If in the above equation the dependence of the second integral upon c_z is ignored, we get the following relation,

$$c_{z\,\max} = k_1 + k_2 R^{\frac{1}{5}}, \quad \cdots\cdots(19)$$

where k_1 and k_2 are constants. If we determine them, so that $c_{z\,\max} = 1.174$ when $R = 1.5 \cdot 10^6$, then

$$c_{z\,\max} = 0.458 + 0.0417\, R^{\frac{1}{5}},$$

while the results of Tôkyô and Pasadena for N. A. C. A. 2412 section can be expressed approximately by

$$c_{z\,\max} = 0.514 + 0.0405\, R^{\frac{1}{5}}$$

which is shown in Fig. 28. From these two equations we see the orders and magnitudes of these constants are in good agreement, hence the author proposes the formula of the above forms —equation (18) or (19)—as the favorable type of formula to express experimental results and for the purpose of extrapolation to higher Reynolds' number in the case of thin aerofoil.

We now proceed to the case of thick or thin

27) M. Ono: On the Frictional Resistance. Journal of the Zôsen-Kyôkwai, October, 1926. also, Masatu-teikô to sono Riron. Journal of the Aeronautical Research Institute, Tôkyô Imperial University, No. 117, 1934.

28) Ergebnisse der Aerodyn. Versuchsanstalt zu Göttingen, 3. Lieferung, page 61.

Fig. 28.
Relation between c_z max and R for N. A. C. A. 2412 Section.

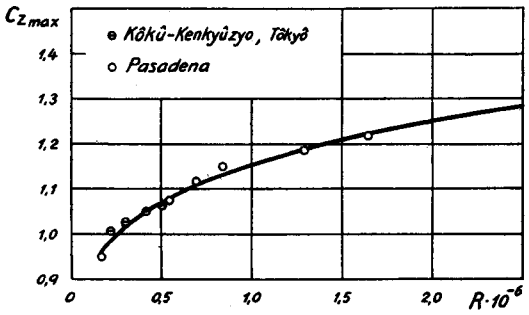

aerofoil but with large camber. As an example easily treated, we take the Joukowski section (Göttingen Nr. 433) again. The square of velocities over the upper surface are shown in Fig. 29. This time the gradient of pressure is much less

Fig. 29.
Computed Values of u_0^2 over the Upper Surface of the Aerofoil.

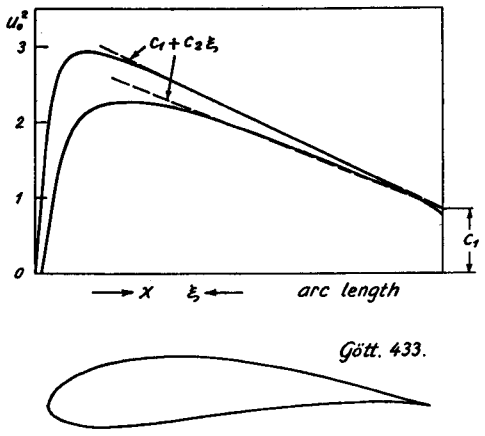

than in the previous example and it is easily supposed that in such aerofoil the position of the transition point from laminar to turbulent is greatly influenced by Reynolds' number.

We integrate equation (14) from the transition point to the trailing edge as equation (17) and as a rough approximation we neglect the second term. If we measure the arc length ξ along the upper surface from the trailing edge, the square of the velocity can be expressed approximately as follows;

$$u_0^2 = c_1 + c_2\xi.$$

The lengths and velocities are hereafter measured, taking the length of chord and the air velocity, far from the aerofoil, as unity, for the sake of simplicity. The constants c_1 and c_2 in the present example are $c_1 \approx 0.86$ and $c_2 \approx 1.12 + 0.94\, c_z$. Hence we get

$$\int_0^{\xi} \frac{du_0^2}{u_0^2} = \log\left(1 + \frac{c_2}{c_1}\xi\right) \quad \text{.....(20)}$$

Now this integral must be equal to a certain constant value in order that the break-away may occur just at the trailing edge. Equating the value of equation (20) to this constant, we can determine ξ_t which gives the position of transition point from laminar to turbulent,

Next we compute the thickness of the laminar boundary layer from the front stagnation point, the velocity distribution in the boundary layer being assumed to be a parabola and calculated in the same way as the turbulent boundary layer. The result can be expressed as follows;

$$\delta = \frac{\Delta}{\sqrt{R}} \quad \text{.....(21)}$$

where Δ is a function of x/t.

Then the Reynolds' number of the boundary layer R_δ which we define as the quotient of the velocity just outside the boundary layer times its thickness and the coefficient of kinematic viscosity, becomes

$$R_\delta = \sqrt{R}\; u_0\Delta \quad \text{.....(22)}$$

The calculated values of $u_0\Delta$ is shown in Fig. 30, and we may express them approximately by straight lines i.e.,

Fig. 30.
Computed Values of $u_0\Delta$ and c_3x.

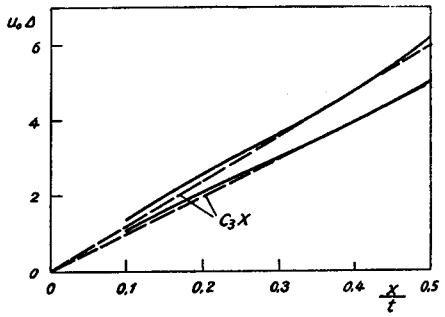

$$u_0\Delta = c_3 x$$

and in the present case $c_3 \approx 3.78 + 6.79\, c_z$.

If we take the critical Reynolds' number $R_{\delta\,cr}$ at the transition from laminar to turbulent layer as equal to 3000, then

$$\sqrt{R}\;(3.78 + 6.79\, c_z)x_t = 3000$$

or

$$x_t = \frac{3000}{\sqrt{R}\;(3.78 + 6.79\, c_z)}, \quad \text{.....(23)}$$

where x_t is the value of x at the transition point. The points defined by x_t and ξ_t must coincide with each other or

$x_t + \xi_t$ = arc length from the front stagnation point to the trailing edge
$= s$.

Putting equation (23) into equation (20) and using

the numerical values c_1, c_2 and c_3, we get the following very approximate relation;

$$1+\frac{c_2}{c_1}\xi_t = 1+\frac{(1.12+0.94\,c_z)}{0.86}(s-x_t)$$
$$=\text{const.}$$

Choosing the constant properly from an example, as in the previous case of thin aerofoil, we get the relation

$$\sqrt{R}\approx 390\frac{c_z+1.19}{(c_z+0.557)(c_z-0.306)}, \quad \ldots(24)$$

and if the magnitude of $R_{\delta cr}$ is varied the constant 390 varies. Taking $R_{\delta cr}$ equal to 2000, 3000 and 4000, such curves represented by equation (24) are shown in Fig. 31 in full lines.

Fig. 31.

Relation between $c_{z\ \max}$ and R.

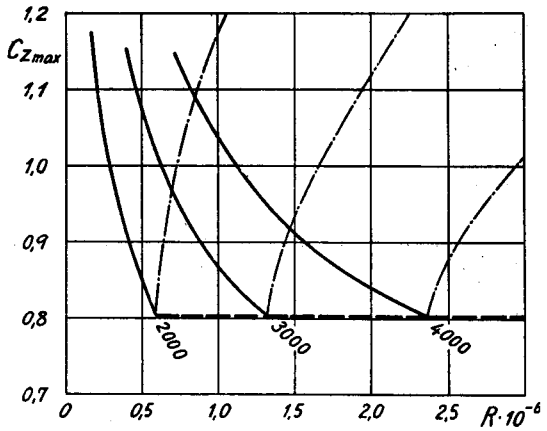

Now equation (24) is valid only when the transition point lies between the point of laminar break-away B and the point of minimum pressure A in Fig. 32a. If the transition point lies before point A as in Fig. 32b, the position of the transition point has no much influeuce upon the break-away as when it lies between A and B, so c_z does not vary much with the Reynolds' number. The condition in which the transition point coincides with point A is expressed from equation (22) as follows;

$$\sqrt{R}\,(u_0\delta)_{\text{at the point of min. pressure}} = R_{\delta cr}.$$

These relations are shown in Fig. 31 in chain lines, taking $R_{\delta cr}$ equal to 2000, 3000 and 4000 respectively.

Fig. 32.

Schematic Diagrams of Flows about a Thick Aerofoil Section.

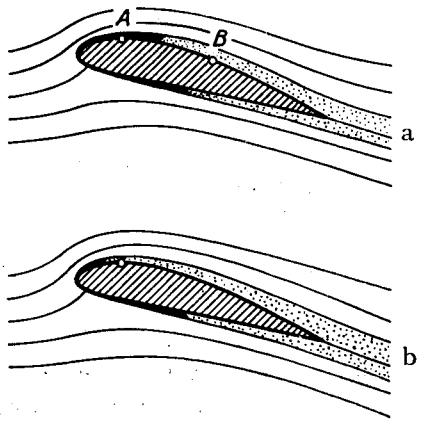

Experiments on thick or large cambered aerofoils show that the lift coefficient yet increases with the incidence angle, even when break-away has already occured near the trailing edge. Hence the above calculated lift coefficient does not give the true maximum lift coefficient, but may be considered proportional to it or nearly so. Moreover at present, the problem of what value $R_{\delta cr}$ should take, how it varies with the conditions of flow i.e. the pressure gradient along the direction of flow and the form of the velocity distribution in the laminar boundary layer are still in obscurity. Hence it is difficult to express the required relation in a single formula. But in this way it may be possible to explain the decrease of the maximum lift coefficient with the Reynolds' number.

Acknowledgment.

In conclusion the author expresses his cordial thanks to the Professors of the Kikwai-Kôgakukwa-Kyôsitu for their kind support throughout the investigations. And special acknowledgment is due to Mr. E. Simomura who had kindly helped the author in executing experiments. Further the author acknowledges his indebtedness to Mr. T. Hirata who zealously assisted the author both in experiments and the dull task of labourious calculation.

(Received January 16, 1935).